Chapter 3

Experimental apparatus

3.1 TRISTAN accelerator

TRISTAN is an e^+ e^- storage ring accelerator at National Laboratory for High Energy Physics(KEK). An overview of the accelerator complex is shown in Fig. 3.1. The TRISTAN accelerator consists of three parts: a liner accelerator(LINAC), an accumulator ring(AR), and a main ring(MR). The length of the LINAC is 400m, and the circumferences of the AR and the MR are 370 m and 3 km, respectively.

First, electrons and positrons are accelerated by the LINAC up to 2.5 GeV and injected to the AR. They are accumulated in the AR and are accelerated up to 8.0 GeV and injected to the MR. These steps are repeated several times to form two bunches of electrons and two bunches of positrons in the MR. Finally, they are accelerated up to ~29.0 GeV and collide every 5.0 μsec at four interaction points(I.P.) in the four straight sections. Three detectors named AMY, TOPAZ, and VENUS, are placed at the I.P.'s as shown in Fig. 3.1. A typical injection time from the LINAC to the MR is about 30 minutes.

The TRISTAN experiment started in 1986 at the center of mass energy($\sqrt{s}$) of 50 GeV. The beam energy was increased gradually by installation of Radio Frequency cavities, and TRISTAN reached the highest energy of 64.0 GeV in 1989. Until the LEP experiment began in this year, TRISTAN was the highest energy e^+ e^- accelerator in the world. From 1990, the data was taken at the center of mass energy of 58 GeV and the TRISTAN experiment aimed at higher luminosity runs rather than at higher energy runs. As shown in Fig. 3.2, a typical integrated luminosity per day became ~800 nb^{-1} at the higher luminosity runs. The TRISTAN experiment ended in May 1995, resulting the integrated luminosity of more than 300 pb^{-1} in total. The data used in this analysis was collected at the higher luminosity runs.

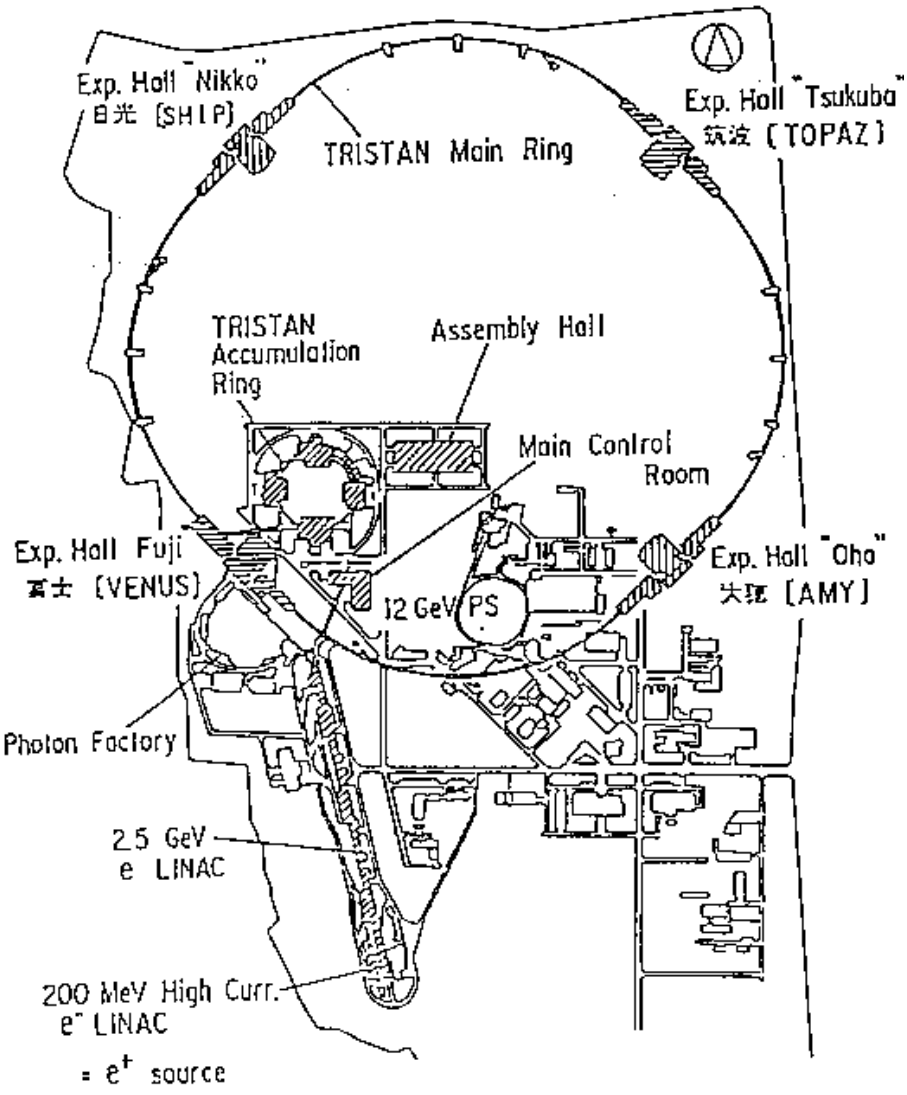

Figure 3.1: An overview of the TRISTAN accelerator system. The TOPAZ detector is located at the Tsukuba experimental hall.

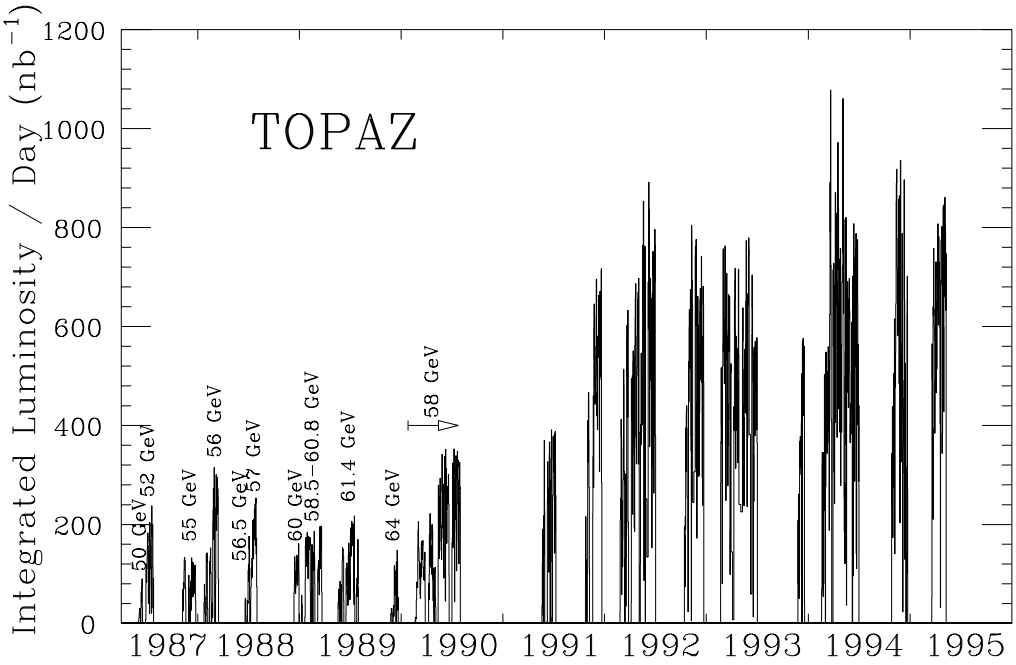

Figure 3.2: The integrated luminosity (nb^{-1}) per day recorded by the TOPAZ detector.

3.2 TOPAZ detector

The TOPAZ detector[37] is general-purpose 4π detector located at Tsukuba experimental hall at north west of the TRISTAN MR. Schematic views of the TOPAZ detector are shown in Fig.3.3. The structure and performance of the TOPAZ detector are summarized in Table 3.1.

The TOPAZ detector was upgraded in 1989 for high luminosity run of TRISTAN. As the results, the TOPAZ detector became a hermetic detector and obtained better measurements of luminosity and charged tracks. The performance of new detector are summarized in Table 3.2.

Charged tracks were detected with a vertex chamber(VTX), a trigger chamber(TCH), and a time-projection chamber(TPC), all of them were placed in an axial magnetic field of 1.0 Tesla. A time of flight counters(TOF) are surrounding the TPC. The energies of photons and electrons were measured with a barrel lead-glass calorimeter(BCL), a end-cap Pb-PWC sandwich calorimeter(ECL), and a forward BGO calorimeter(FCL). The details of major detector components are described below.

The coordinate system of the TOPAZ detector used throughout this thesis is

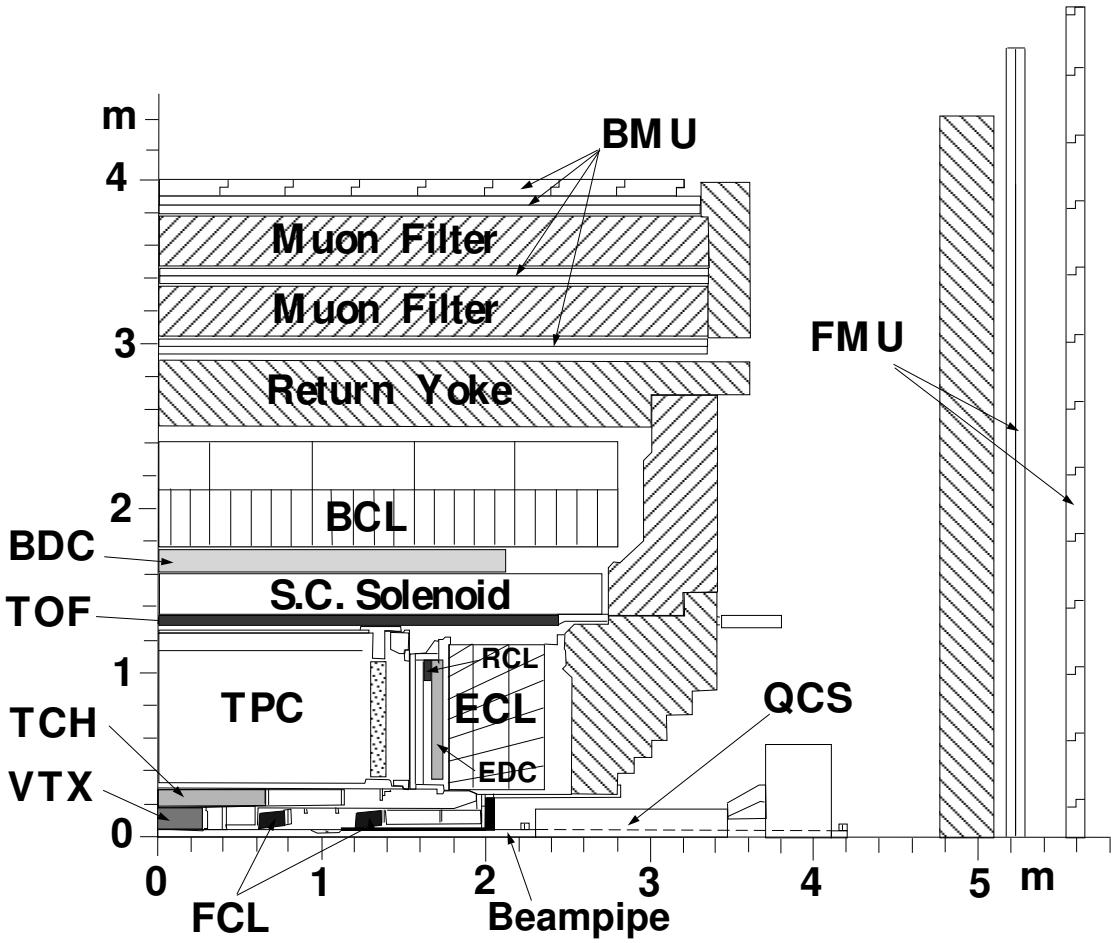

Figure 3.3: Schematic views of the TOPAZ detector.

Components	Material and Size	Measured Performance
beam pipe	0.2m(ϕ) 1.8mm-thick Al	
IDC	Cylindrical 10 layers	$\sigma_{r\phi} = 220\mu$m $\sigma_z = 15\mu$m
TPC	2(Z) $\times$ 8 sectors 175 wires, 10 pad lows / sector 512 pads / sector 364 < r < 1090 mm,L = 2.2 m	$\sigma_{r\phi} = 206\mu$m $\sigma_Z = 335\mu$m $\sigma_{dE/dx} = 4.6\%$ $\sigma_{P_T}/P_T = \sqrt{(1.5P_T)^2 + 1.6^2}$ %
TOF	64 plastic scinti. (BC412) $\lvert\cos\theta\rvert < 0.85$	$\sigma_{time} = 210$ps
Magnet	2.9 m(ϕ) $\times$ 5m(L),0.7X_0	B = 1.0 T
BDC	Streamer tube 4 layers(rϕ)	$\sigma_{r\phi} = 350\ \mu$m
BCL	Pb-glass (SF6W),20 X_0 4300 blocks $\lvert\cos\theta\rvert < 0.848$	$\sigma_E/E = \sqrt{(8.0/\sqrt{E})^2 + 2.5^2}$ % $\sigma_\theta = 0.38°$
BMU	3 layers (rϕ) + 1 layers (Z) $\lvert\cos\theta\rvert < 0.75$	$\sigma_{r\phi} = 1$mm
LUM	Pb-scinti. Sandwich 38 mrad < θ < 66 mrad	$\sigma_E/E = 3.5$ % (for 26 GeV electron)
EDC	Streamer tube 2 layers each in x and y.	
ECL	Pb-PWC sandwich 18 X_0 thick $0.848 < \lvert\cos\theta\rvert < 0.978$	$\sigma_E/E = 6.7$ % (for 25-30 GeV electron) $\sigma_\theta = 0.7°$

Table 3.1: The performance of the TOPAZ detector components.

Components	Material and Size	Measured Performance
beam pipe	0.1m(ϕ) 1.3mm-thick Be in $\|z\| < 15$ cm	
VTX	Jet-Type 25 sense wires/layer $\times$ 8 layers	$\sigma_{r\phi} = 30 \sim 50\mu$m
TCH	Cylindrical 128 sense wires/layer, 8 layers	$\sigma_{r\phi} = 250\mu$m
EMU	3 layers (rϕ) + 1 layers (Z) $\|\cos\theta\| < 0.75$	$\sigma_{r\phi} = 1$mm
FCL	BGO + Si, 21 X_0 thick $0.848 < \|\cos\theta\| < 0.978$	$\sigma_E/E = 5.0$ % (for 28 GeV electron)
RCL	W-Si sandwich, 18 X_0 thick $0.82 < \|\cos\theta\| < 0.87$	$\sigma_E/E = 20$ % (for 28 GeV electron)

Table 3.2: The performance of new detector components.

defined as shown in Fig. 3.4: z is the beam-electron direction; x is the horizontal axis; and y is the vertical axis.

3.2.1 Time-Projection Chamber(TPC)

The Time-projection chamber(TPC)[38] is the central tracking device of the TOPAZ. The TPC provides simultaneous measurements of three dimensional position and energy loss(dE/dx) of charged particles to be used for particle identifications. The TPC is also used for the trigger of charged tracks(TPC trigger). The schematic view of the TPC is shown in Fig.3.5.

The axial length of the sensitive volume is about 2.0 m in z-direction and the inner and outer radii are 0.3 and 1.1 m, respectively. The TPC consists of 8 multiwire proportional chambers (sector:shown in Fig.3.6) located at each endcap side and a cylindrical pressure vessel.

Each sector has 175 anode sense wires, 175 field wires spacing 2mm alternatively, and 10 pad rows (512 pads per one sector) on the cathode plane. The sense wires are held at 1970V and the field wires at 200V under the normal condition, respectively. The vessel is made from the Glass Fiber Reinforced Plastic(GFRP) and filled with a gas mixture of 90% Ar and 10 % CH_4 at 3.5 atm.

Charged particles passing through the TPC sensitive region ionize gas molecules and liberate electrons along their trajectories. These dissociated electrons drift

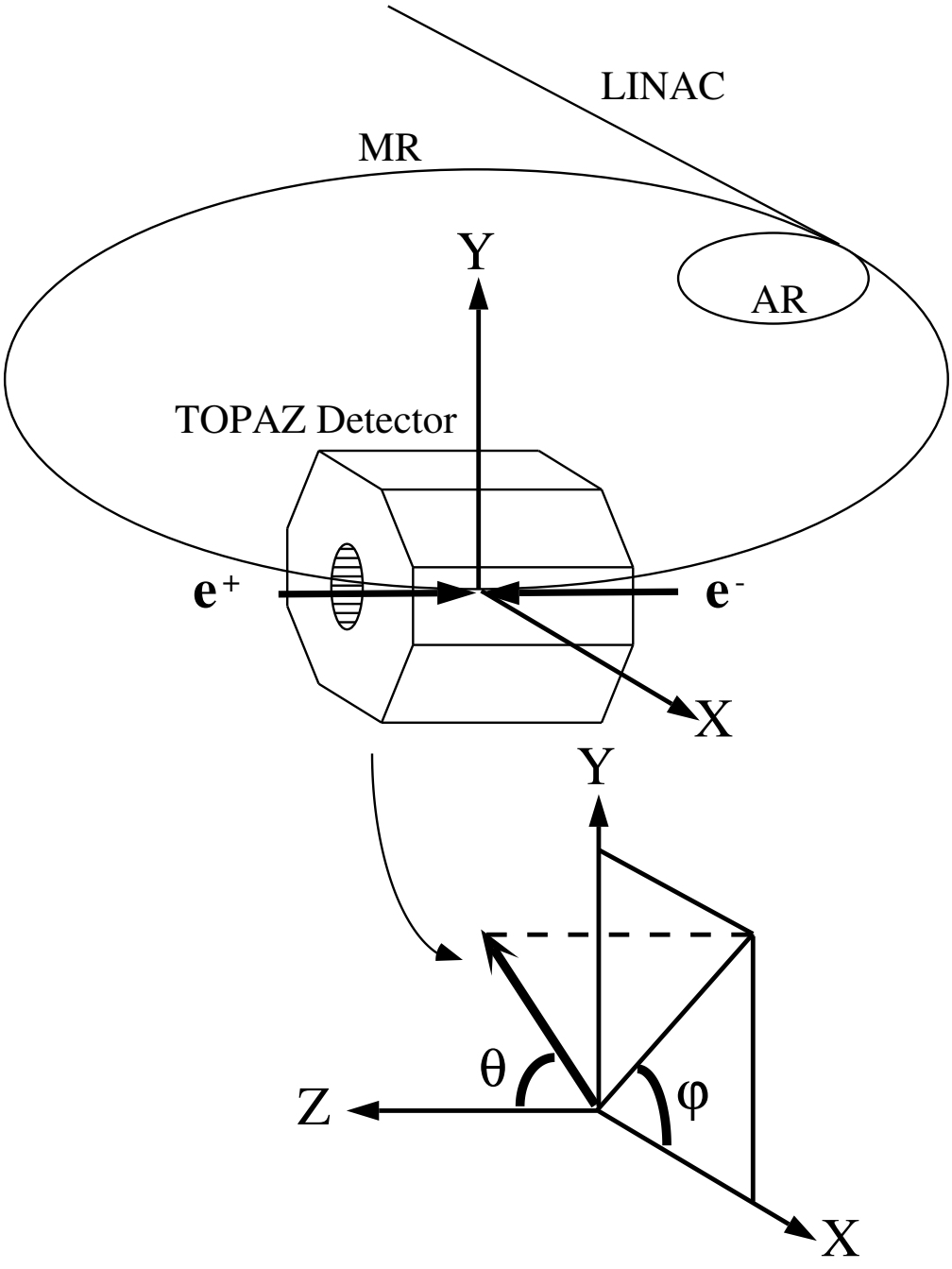

Figure 3.4: Coordinate system of the TOPAZ detector.

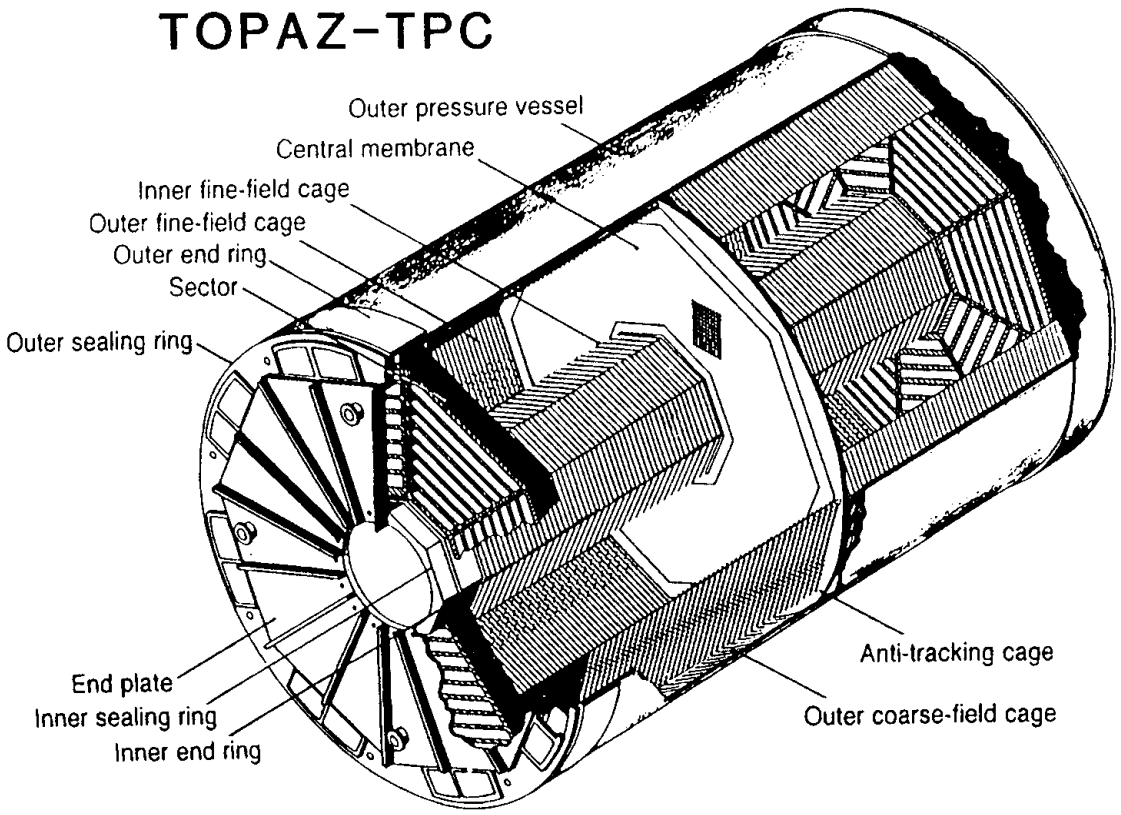

Figure 3.5: A schematic view of the TPC.

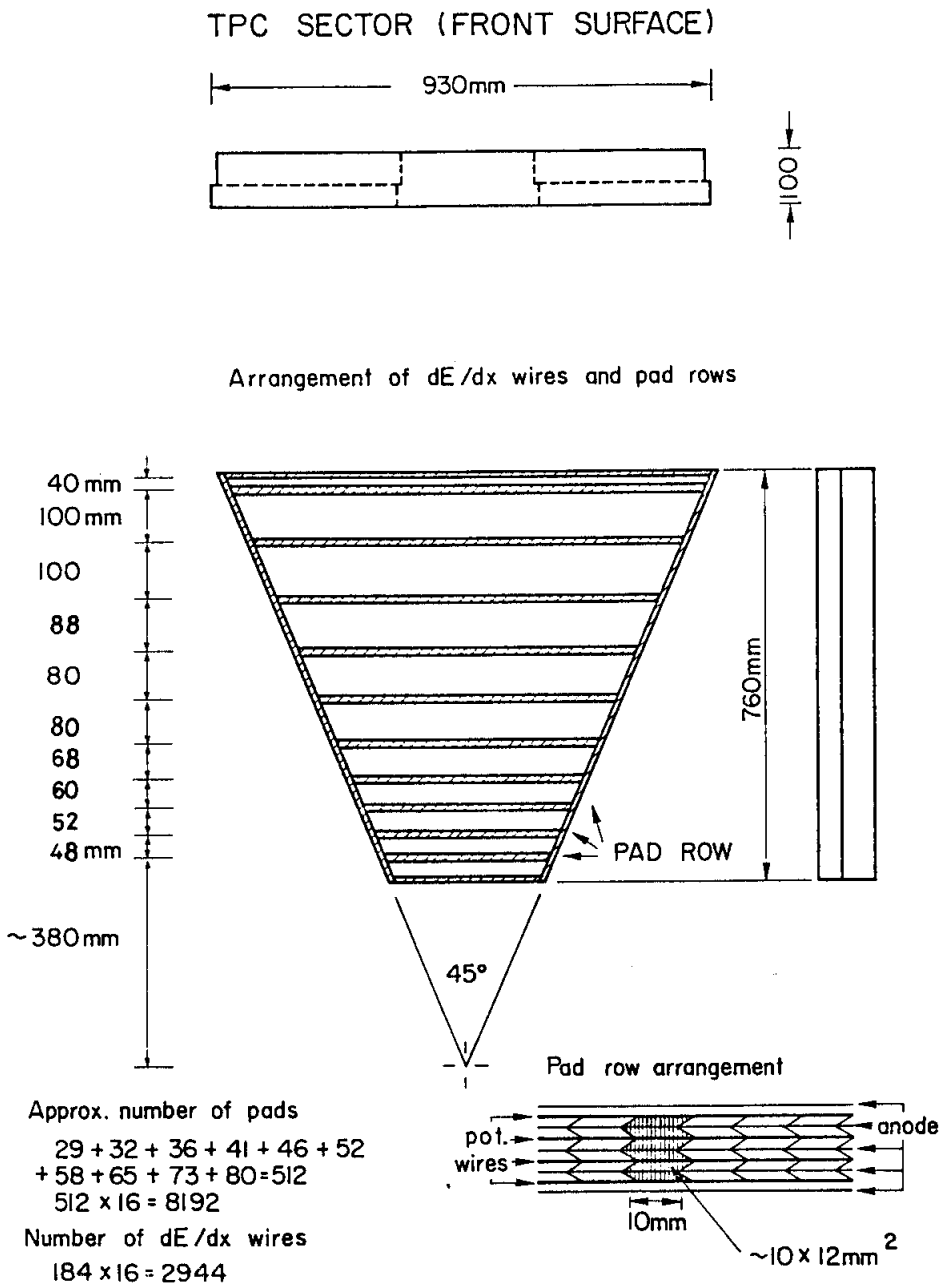

Figure 3.6: The TPC sector.

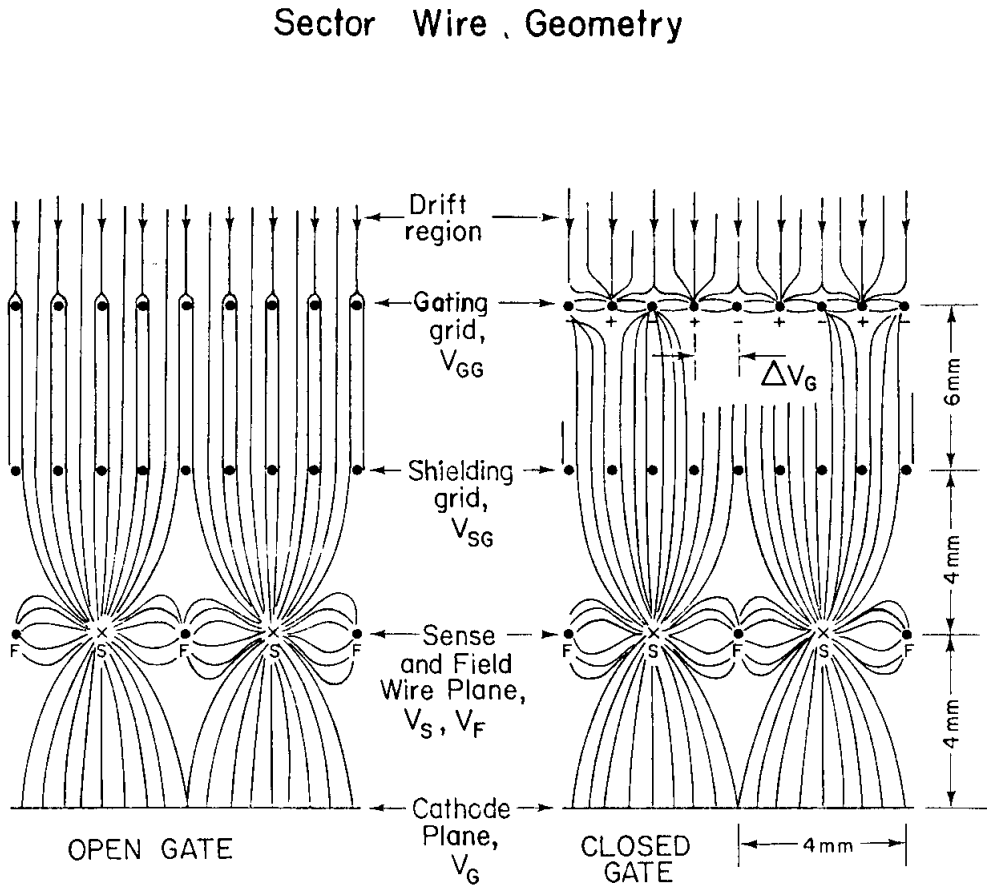

Figure 3.7: The gating grid of the TPC sector.

along the direction of the electric field of 353 V/cm toward the sectors at a typical speed of 5.3 cm/μsec. This electric field is produced by supplying the negative voltage to the central membrane located in the center of the pressure vessel. These electrons finally produce avalanches around sense wires. The ion clouds produced there induced electric signals on the nearby cathode pads. The signals from wires and pads are amplified and are shaped by analogue electronics. They are then fed into charge coupled device (CCD) digitizers sampling the wave-forms in units of a 100 nsec "bucket" from which the z-positions and energy-loss (dE/dx) information are extracted. The gains of the wire signals are calibrated by the X-ray (5.9 keV) from the ^{55}Fe sources.

Since the positive ions moves 10^4 times slower than electrons do, they would build up a positive ion clouds in the TPC sensitive region and would cause a distortion of the electric field (space charge effect). In order to reduce such an effect, the gating-grid plane is placed above the shielding-grid plane (Fig. 3.7).

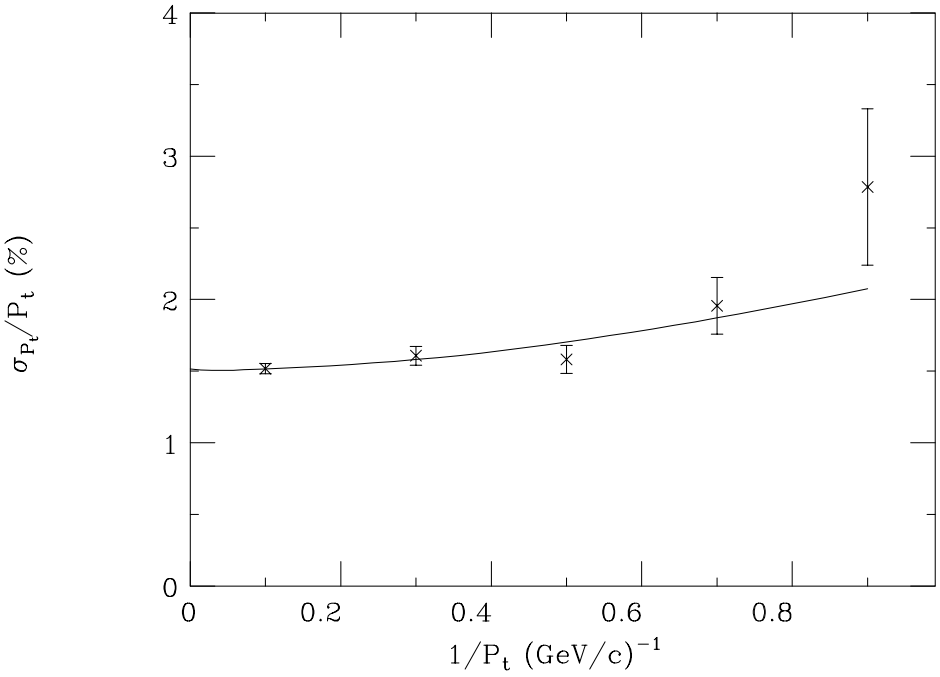

Figure 3.8: Momentum resolution of the TPC as a function of P_T.

The gating grids are usually closed to prevent positive ions from drifting to the sensitive region and are opened only when the opening signals come from other detectors (i.e., trigger system).

The spatial and momentum resolutions are studied with cosmic rays as well as Bhabha and $\mu^+\mu^-$ events. The spatial resolution was obtained to be σ_{xy}=185μm and σ_z=335μm. By comparing two measurements in the opposing sectors in cosmic-ray events, the momentum resolution was measured to be

$$\sigma_{P_T}/P_T = \sqrt{(1.5P_T)^2 + 1.6^2}\%.$$

The momentum resolution as a function of momentum is shown in Fig. 3.8. The dE/dx resolution was studied using minimum-ionizing pions in the beam events. The obtained resolution is $\sigma_{dE/dx}$ =4.6% after all calibrations such as gas density corrections and drift-path length corrections.

3.2.2 Trigger chamber(TCH)

The trigger chamber is located outside the VTX. The purpose of this chamber is to provide a fast trigger signal and to help track linking between the VTX and the TPC. The TCH consists of 8 layers of sense wires which are azimuthally segmented into 128 cells per layer. The shape of each cell is hexagonal and the size of the

cell is about 1 cm. It is filled with the HRS gas [Ar(89%)/CO_2(10%)/CH_4(1%)] at 1 atm.

The spatial resolution, momentum resolution, and chamber efficiency are studied with cosmic ray events. The position resolution was obtained to be $\sigma_{r\phi} = 250\mu$m, and momentum resolution was approximated by

$$\sigma_{P_T}/P_T = \sqrt{(33P_T)^2 + 0.6^2}\%.$$

The chamber efficiency and the trigger efficiency are 98% and 99.8% under a normal condition, respectively.

3.2.3 Time of flight counter(TOF)

A time of flight counter(TOF)[39] consists of 64 plastic scintillators, each 4 m long, 4.2 cm thick, and about 13 cm wide, which are cylindrically placed surrounding the TPC. The scintillator cross section in tapered so as to leave as little space as possible between adjacent scintillators. Each end of the scintillator is viewed by a photomultiplier via a light guide. The TOF is intended both to identify some of the particles produced by e^+e^- collisions and to provide a trigger signal for data taking (charged pre-trigger).

The average time resolution of the TOF system is estimated to be 210 psec based on measurements using a test beam on the KEK proton synchrotron.

3.2.4 Barrel Calorimeter (BCL)

The Barrel Calorimeter (BCL)[40], which comprises 4300 lead-glass Čerenkov counters, has a cylindrical structure covering an angular region of $|\cos\theta| \leq 0.82$. The calorimeter is divided into 72 modules of identical shape, 8 in the ϕ (azimuthal) direction and 9 in the z direction as shown in Fig.3.9. Each module consists of a matrix of 12(ϕ)×5(z) lead-glass counters allowing room for the service port (chimney) for the superconducting solenoidal magnet.

Each lead-glass counter is made of SF6W and has 20 radiation lengths (X_0), so that it can absorb more than 95% of the shower energies at TRISTAN's highest energy. The lead-glass blocks are tilted by 1.8° with respect to the radial line in the $r-\phi$ plane so that no photons coming from the interaction point escape through the counter-to-counter gaps. The Čerenkov light emitted in a lead-glass counter is detected by a photomultiplier after passing through a light guide. The signal from the photomultiplier is sent to a charge sensitive ADC and is also used for a neutral trigger. The system is calibrated by using a Xe flash lamp.

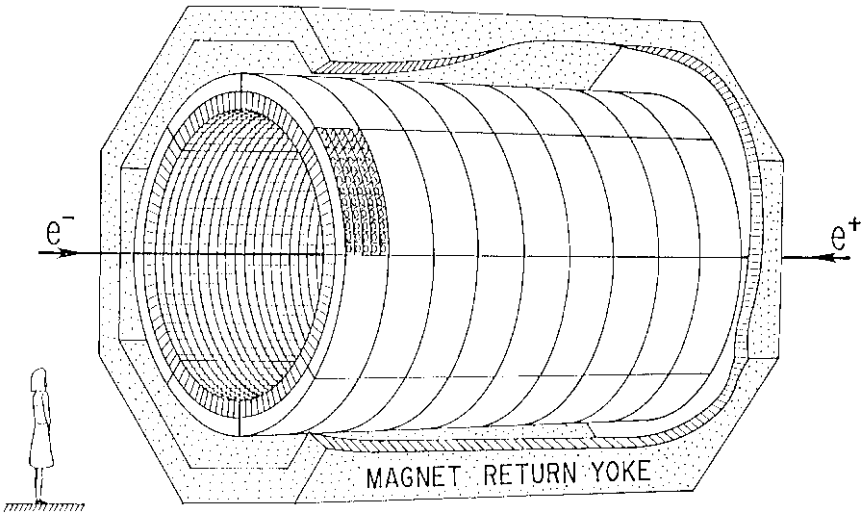

Figure 3.9: Schematic view of the Barrel lead-glass Calorimeter

The performance of the BCL was studied by using Bhabha events. Fig. 3.10 shows the energy distribution for Bhabha events at $\sqrt{s} = 52$ GeV. The energy and spatial resolution were determined to be $\sigma_E/E = \sqrt{(8/\sqrt{E})^2 + 2.5^2}\%$ (E in GeV) and σ_θ=0.38°, respectively.

3.2.5 End-cap Calorimeter(ECL)

The end-cap calorimeter(ECL)[41], mounted in each end-cap, is a gas sampling electromagnetic calorimeter covering an angular region of $0.85 \leq |\cos\theta| \leq 0.98$. It consists of proportional wire tubes interleaved with lead absorbers, and is operated with the gas mixture of 95% Ar and 5% CH_4. The ECL is segmentated into 3 modules along the beam direction; the first module comprises 8 layers with 2 mm lead absorbers, the second 12 layers and the third 14 layers with 3 mm absorbers, amounting to $18X_0$. One layer is made of 196 high resistive plastic tubes glued on a printed circuit(PC) board. Each of the plastic tubes has a cross section of 10×15 mm^2.

The energy distribution for Bhabha event at $\sqrt{s}$=52 GeV is shown in Fig. 3.11, and the energy resolution was obtained to be $\sigma_E/E = 6.7$ %. The polar angle resolution was measured to be $\sigma_\theta = 0.7°$.

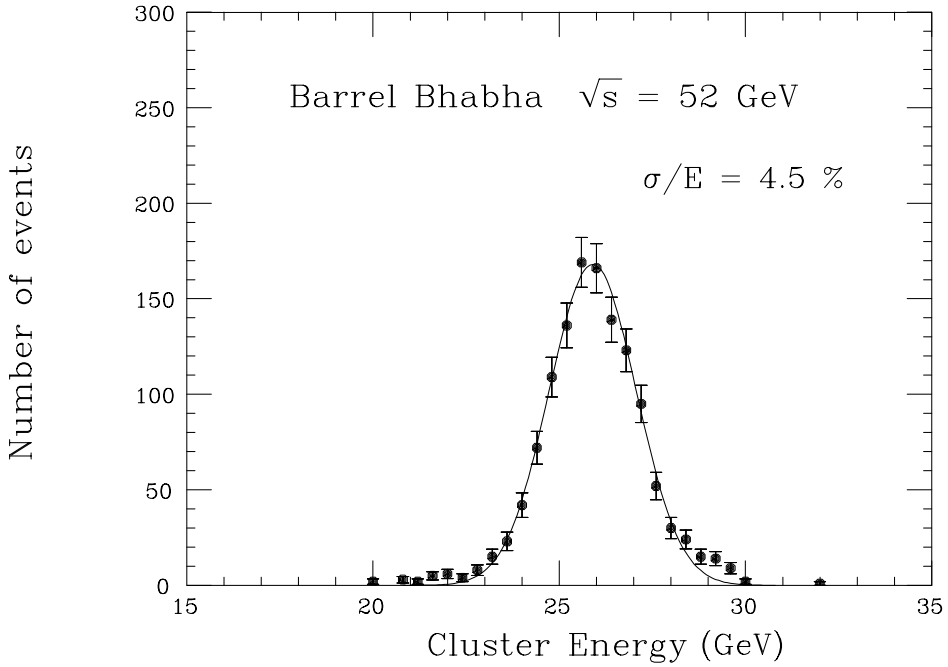

Figure 3.10: Energy distribution for Bhabha events observed with the BCL at center of mass energy of 52 GeV.

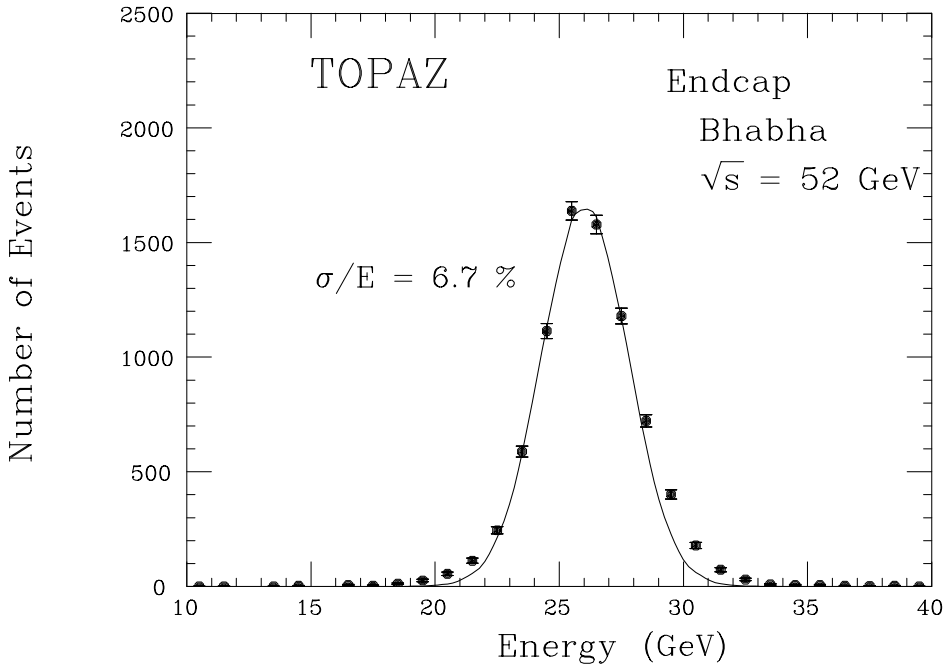

Figure 3.11: Energy distribution for Bhabha events observed with the ECL at center of mass energy of 52 GeV.

3.2.6 Forward Calorimeter(FCL)

The TOPAZ detector was upgraded in order to achieve improved performance for high luminosity e^+e^- experiment. The forward calorimeter (FCL)[42] is one of the important components of new detectors which located at a small angular region (which covers polar angles from 3.2° to 13.6°) of the TOPAZ detector. The main purpose of FCL are follows: (1)To make the TOPAZ detector hermetic; (2) To tag electrons and/or positrons in order to study two-photon processes in detail; (3) To monitor the real time luminosity, and to measure the integrated luminosity of TOPAZ detector precisely. The old TOPAZ luminosity monitor[43] was replaced with this new FCL in 1989.

The structure of the FCL is schematically shown in Fig. 3.12. It comprises four identical modules, the two modules at $z = \pm 60$cm called the forward-backward calorimeter (FBC) and the other two modules at $z = \pm 12$cm the luminosity monitor (LUM) for convenience. Each module is azimuthally segmented into twelve blocks, as can be seen in Fig. 3.13. Each block comprises a BGO calorimeter for energy measurements, and a silicon strip detector located in front of the BGO calorimeter for position measurements. The BGO calorimeter consists of 5.3 mm thick tungsten absorber ($1.5X_0$), 150 mm thick BGO crystal($13.5X_0$), and a silicon photodiode readout system.

The energy resolution of the BGO calorimeter is less than 5% from 1 to 30 GeV which was estimated by test beam measurements carried out at the IT4 test beam line of the AR and Bhabha electrons. The silicon strip detector is designed so as to keep the polar angular resolution within 5%.

3.3 Trigger system

The role of the trigger system is to detect physical events effectively from huge backgrounds.

The trigger scheme for the TOPAZ detector[44] is slightly different from other *standard* detectors. Raw-data sizes of the TOPAZ detector are 100Kb/event for hadronic events and 20Kb/event for two-prong events. In order to achieve a dead time of less than 10%, a total trigger rate of less than 3 Hz is necessary. Still, the huge backgrounds from the beam-gas scattering are not removed without using the rz tracking, which takes about 24 μs, i.e. the drift time of ionizing electrons. Also, the frequency of the TPC's gating grid pulsing should be reduced in order to minimize the distortion effect. Thus the TOPAZ trigger is exacted in multiple steps. The first step called *Pre-trigger* is done within the period between two

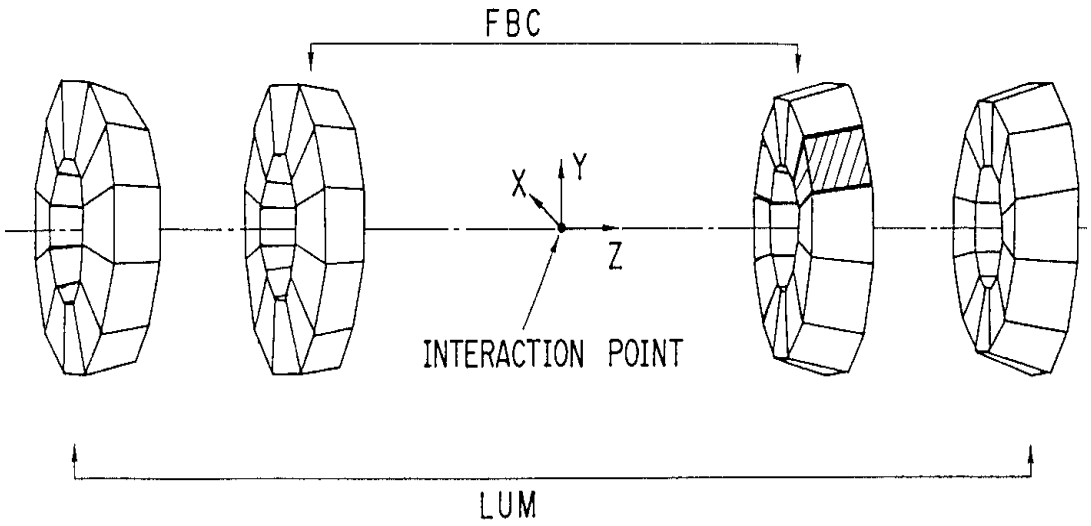

Figure 3.12: Schematic view of the forward calorimeter.

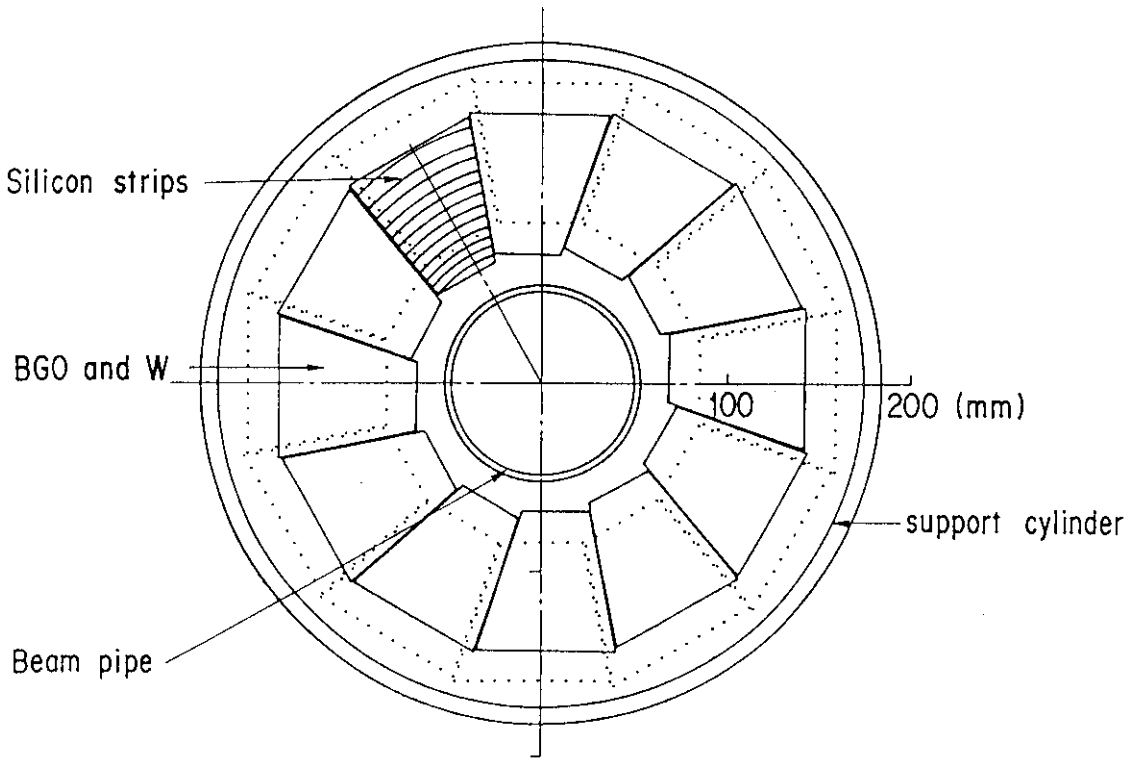

Figure 3.13: Shape of a module viewed from the beam axis.

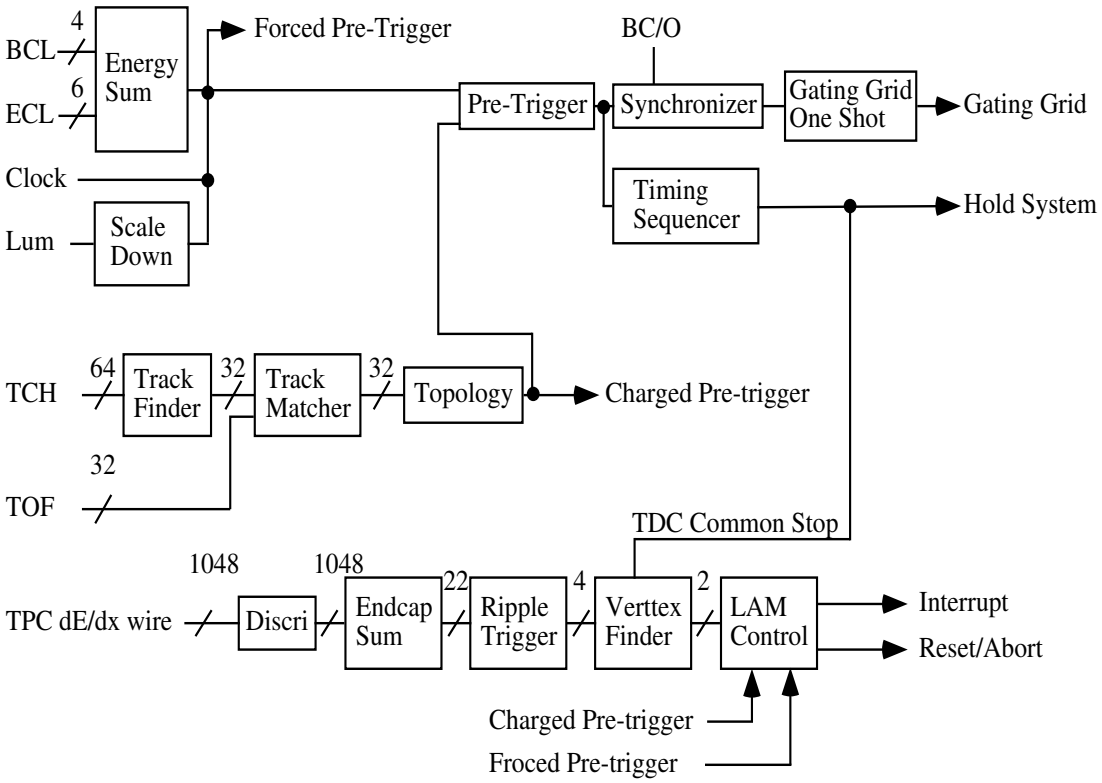

Figure 3.14: Trigger scheme.

successive beam crossing signals (BC/O), which is 5μsec for 2-bunch operation. The rate is about a few hundred Hz at this level. The second step is done by the TPC, which is called *Trigger*, takes about 30 μsec.

The whole scheme is shown in Fig.3.14. There are two branches in *Pre-trigger* line, an energy trigger (*Forced Pre-trigger*) and a track trigger (*Charged Pre-trigger*). The *Forced Pre-trigger* and the *Charged Pre-trigger* are ORed and synchronized with BC/O. The gating grid of the TPC is pulsed by these *Pre-trigger*s. If this first level decision is not generated, all the ADC's and TDC's are cleared before the next BC/O.

The TPC trigger starts at the *Pre-trigger* timing. After electrons drift to the TPC wire plane, the TPC trigger issues either *Trigger* or *Reset/Abort* (R/A) to the whole on-line system. The *Forced Pre-trigger* is treated as a *Trigger* (an energy trigger) without any other condition. The events are recorded when the *Trigger* comes from the TPC trigger or the energy trigger. When the R/A signal arrives, the whole on-line system is reset and becomes ready for the next event. The timing chart is shown in Fig.3.15.

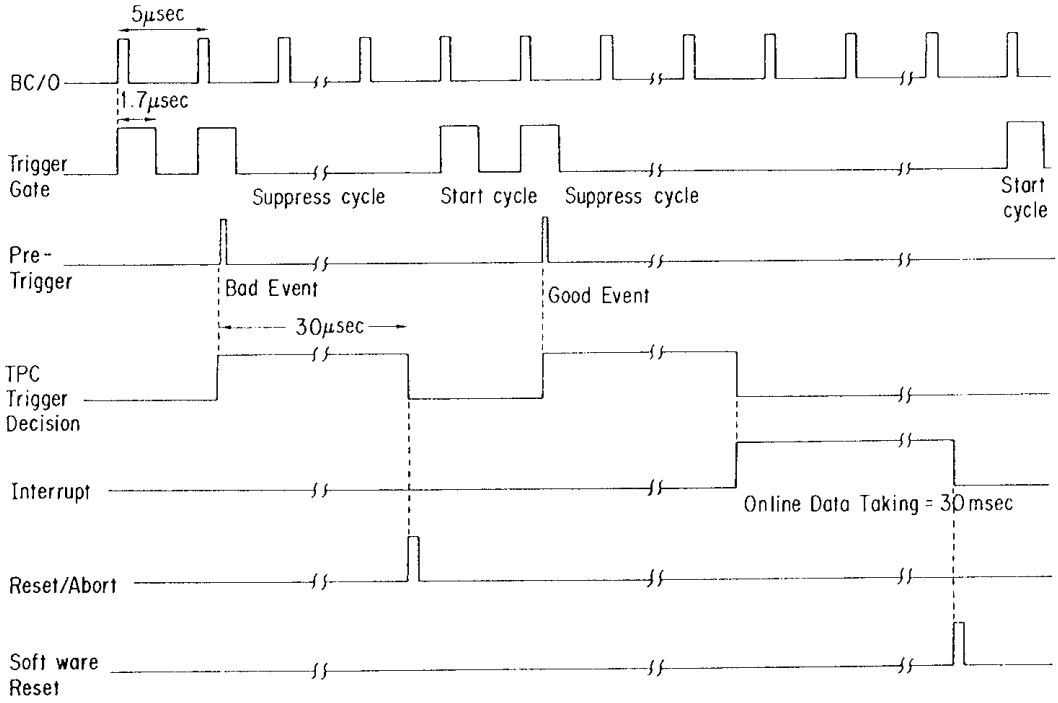

Figure 3.15: Trigger timing chart.

3.3.1 Energy trigger

The energy trigger is designed mainly for Bhabha events, hadronic events, and two-photon events. The BCL and the ECL energy sum signals are processed by the energy sum modules and makes the energy trigger signals. The BCL, which consists of 4300 lead glass counters, are grouped into three z slices; i.e. forward, center, and backward. The total energy in each slices is called the *Partial Sum*. The *Total Sum* of the BCL is the sum of these three *Partial Sum*. The ECL has also four summing outputs, the inner and outer cylinders of both end-caps, those are also called *Partial Sums*. The sum of the ECL signals from both end-caps makes the *Total Sum*.

As shown in Fig.3.16, the Energy trigger is generated by OR's if following conditions:

- The *Total Sum* of the BCL $>$ 4 GeV (2 GeV);
- The *Total Sum* of the ECL $>$ 10 GeV;
- At least 2 *Partial Sums* of the BCL $>$ 1 GeV;
- Both ends have the *Partial Sums* of the ECL $>$ 3 GeV; and

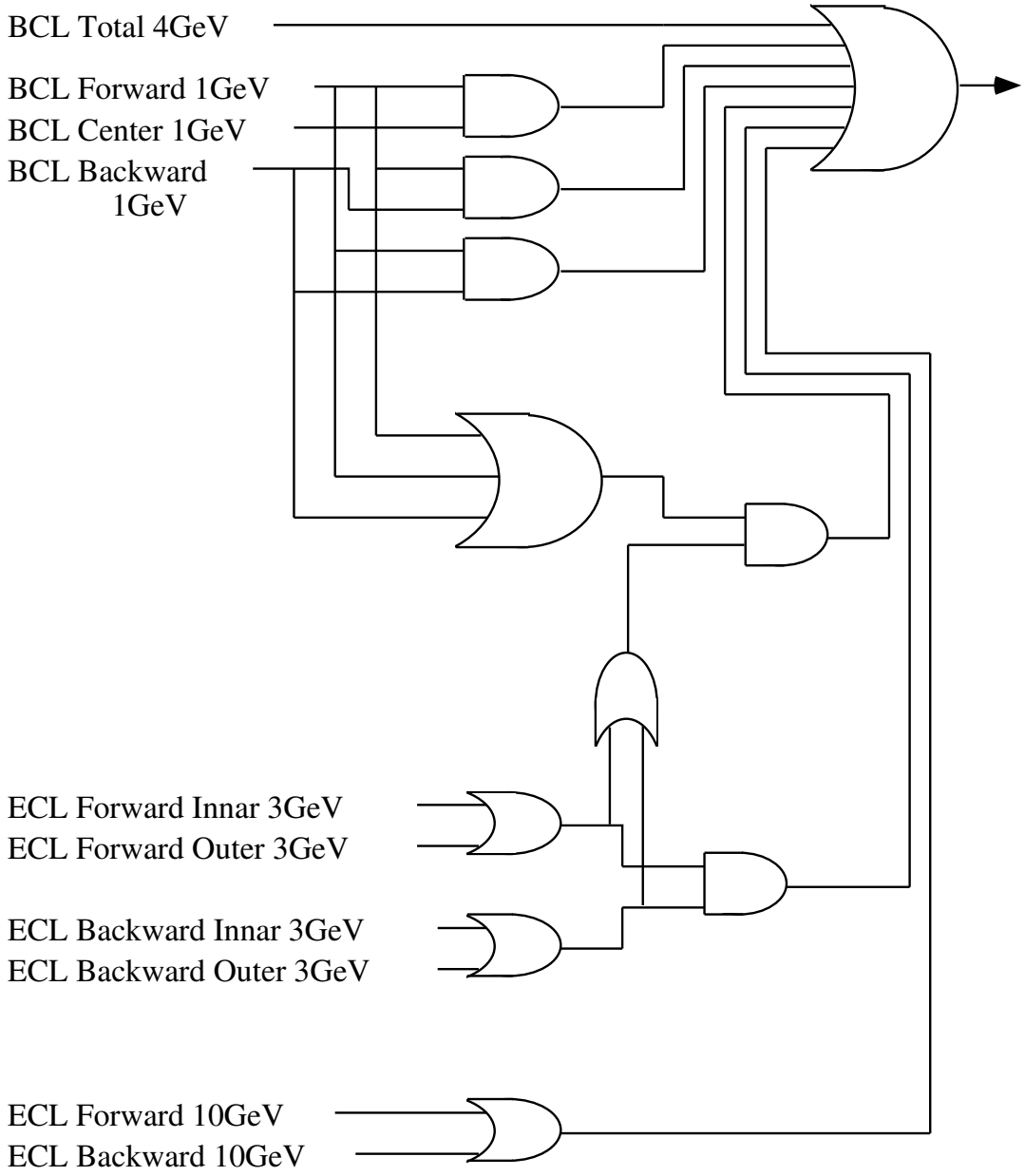

Figure 3.16: A block diagram of the energy trigger.

- At least 1 *Partial Sum* of the BCL $>$ 1 GeV and at least 1 *Partial Sum* of the ECL $>$ 3 GeV.

To detect single-photon production events, the energy level for discriminations was set to 2 GeV for the *Total Sum* of the BCL in 1992. The typical rate during a beam experiment at $\sqrt{s} = 52$ GeV was 1.4 Hz in total.

3.3.2 Track trigger

The track trigger is designed to accept low multiplicity events with little calorimeter energy deposit, such as $e^+e^- \rightarrow \mu^+\mu^-$ and two-photon events. It consists of two steps; the pre-trigger and the TPC trigger.

Track pre-trigger

The track pre-trigger requires coincidence hits in the TCH and the TOF counter at the timing of BC/O. The TCH is azimuthally segmented into 64 subsectors. Each sector has a track finder based on the *table look-up* method, using a 16K SRAM. A P_T-dependent mask is down-loaded by an on-line computer via a FASTBUS/CAMAC dataway. In the trigger decision, the 64 outputs from the track finder are ORed into 32 sectors. There are 64 TOF counters surrounding the TPC pressure vessel. The hit information in two adjacent counters is ORed to provide 32 sector signals. The pre-trigger recognizes the "charged-track" when the one hit in the TCH sector has a corresponding hit in the TOF counter as shown in Fig.3.17. The condition 1/32:3/32 means that one TCH sector is corresponded to the three TOF sectors, the azimuthally same one and both side of the adjacent ones. This condition determines a minimum acceptable P_T of a charged track since a low P_T track cannot hit the adequate region in the TOF. From the cosmic ray test, the charged track with $P_T >$ 0.3-0.7 GeV/c, depending the TCH-TOF combination, is triggered (discussed later).

The pre-trigger is generated when at least two back-to-back track segments are found in the TCH (Fig.3.17). Each 32 sectors of TCH and TOF is paired into 16 sectors. The condition 1/16:7/16 means that "back-to-back" is defined to have one track segment in the TCH and another one in the seven TCH sectors, the opposite one and both side of the adjacent three's. This opening angle cut is effective to reject the spiral electron backgrounds. The opening angle condition in the used data was set to be greater than 45-70^o, depending on beam conditions.

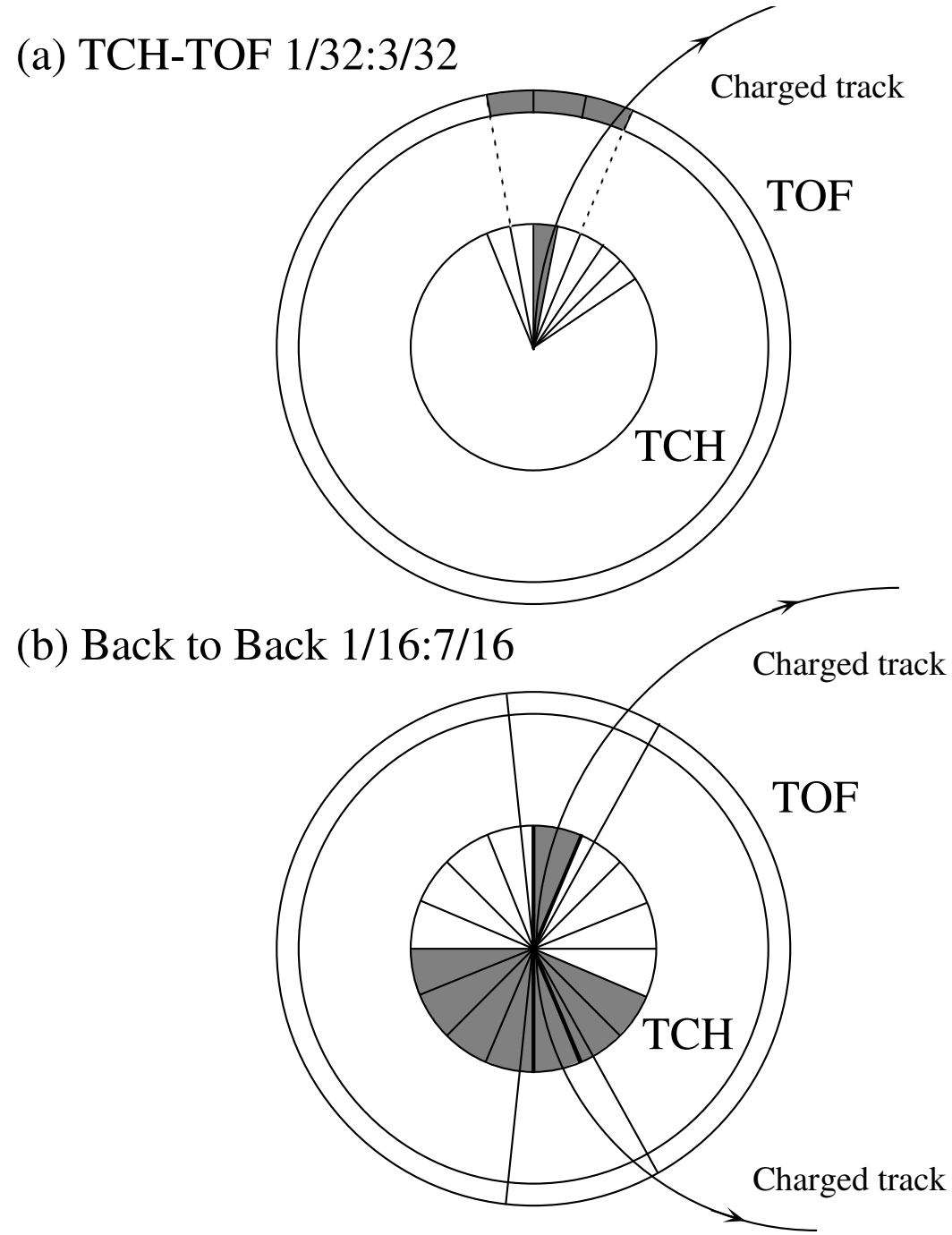

Figure 3.17: The principles of the track pre-trigger.

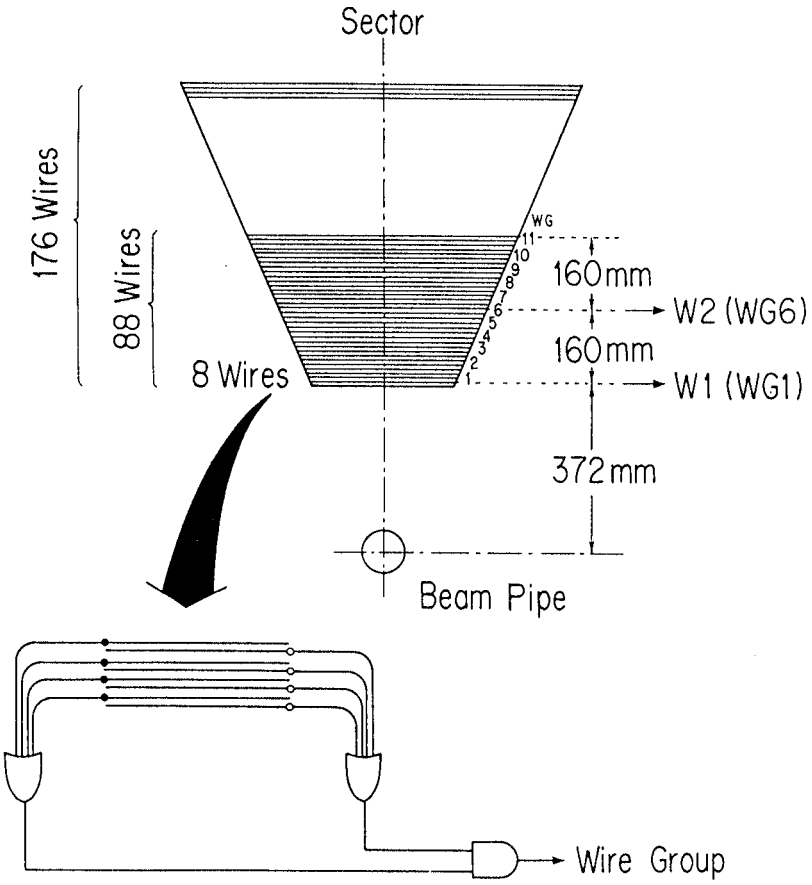

Figure 3.18: The sector dE/dx wire configuration.

TPC trigger

The TPC trigger requires that there are two or more tracks in the r-z projection which are extrapolated to the vicinity of the interaction point[44]. The TPC trigger consists of a *Ripple Trigger*, a *Vertex Finder*, and a *LAM Controller*.

Each TPC sectors has 176 sense wires. Out of these, 88 wires close to the beam line are used. The 8 adjacent wires are grouped. In each group, the outputs of 4 alternating wires are ORed and the resulting two outputs are ANDed, as shown in Fig.3.18. Corresponding wire groups are ORed in each endcap unit (8 sectors/endcap), so that 11 wire groups are available in TPC sector. These signals are processed by the *Ripple Trigger*. In the *Ripple Trigger*, the trailing edge of each signal is stretched by a one-shot of 1 μs. In principle, 10 successive overlaps are required in the logic, as shown in Fig.3.19.

The tracks recognized by the *Ripple Trigger* are processed by the *Vertex Finder*. Using the two timing signals, W1 and W2 in the Fig.3.19, the track

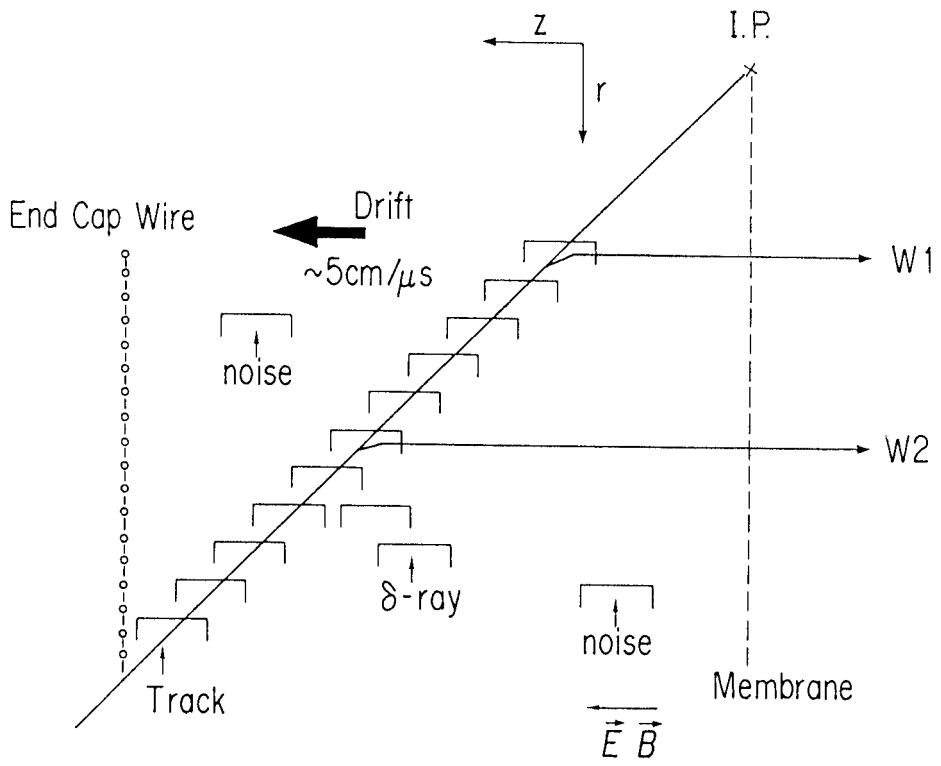

Figure 3.19: Principle of the *Ripple Trigger*.

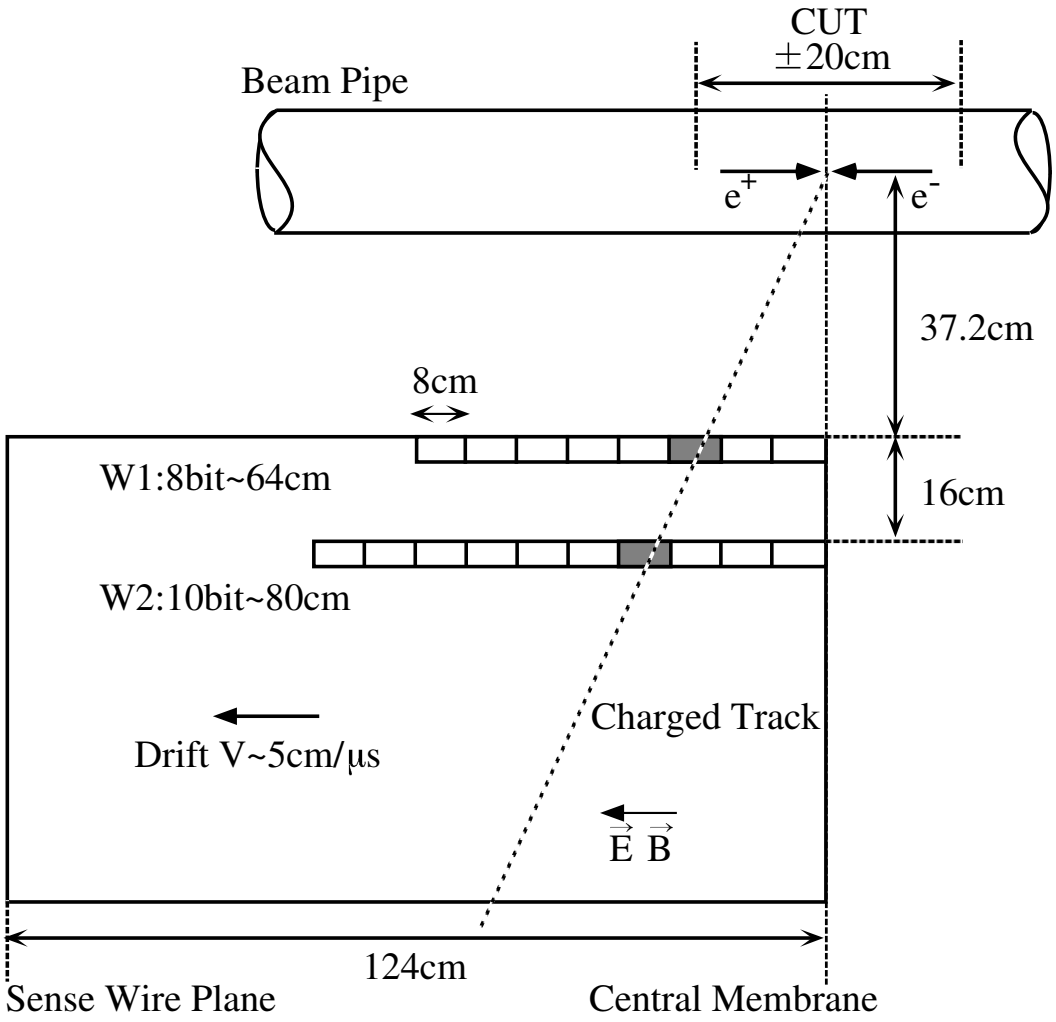

Figure 3.20: Principle of the *Vertex Finder*.

is extrapolated to the interaction point. The calculation was done using the *Vertex Finder*. Fig.3.20 shows the principle of this module. The *Vertex Finder* is based on the clock TDC and 256K SRAM (18 bit address). The current vertex cut is ±20 cm in the beam direction. This vertex finding is essential in rejecting huge beam-gas backgrounds.

After the track selection, the *LAM controller* performs the last decisions. When an event is accepted by the *Forced Pretrigger* or two sector hits (not adjacent) in the TPC *Vertex Finder*, an interrupt signal is generated and the on-line computer starts data-taking, otherwise the Reset/Abort signal is sent to the whole system so that the system become ready for the next event. The rate of the TPC trigger is 2 $\sim$ 6 Hz, and the dead time is 5 $\sim$ 10%, depending the beam condition.

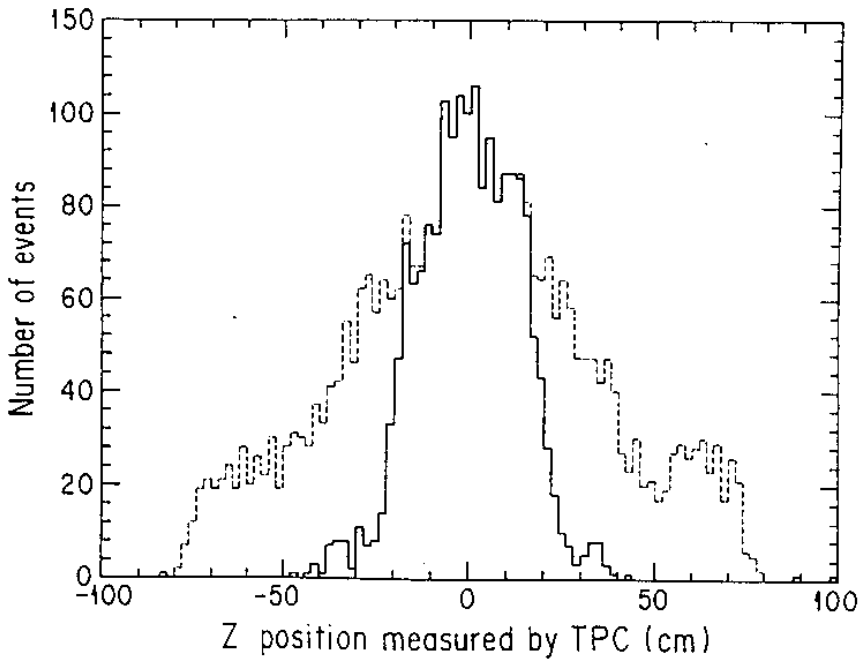

Figure 3.21: The z distributions of the tracks in the triggered events with (solid-line) and without (dashed-line) the software trigger.

Software trigger

To improve the z resolution of the TPC trigger, the software trigger was installed as a part of TOPAZ trigger system in 1990[44]. The software trigger consists of four microprocessors and other interface cards including TDCs in a signal VME crate.

The 32 timing signals (W1 and W2 from each TPC sector) used to find the vertex in the TPC trigger are read by the TDCs and more precise vertex reconstruction is done by the microprocessors. The TDC has a 25.6 μsec dynamic range with a 100 nsec resolution. This gives a track coordinate with a spatial resolution of 5 mm in the z direction. The double pulse resolution of the timing measurement is 1.5 μsec, which provides a double track resolution of 7.5 cm.

Fig.3.21 shows the z distributions of the tracks in the triggered events with (solid-line) and without (dashed-line) the software trigger. These distributions are measured with cosmic ray events. The vertex constraint was tighten significantly by the software trigger. This software trigger reduced the rate of the track trigger down to 30$\sim$40% with 0.5% inefficiency.

3.3.3 New trigger logics

In spring 1992, two new trigger logics were installed in the TOPAZ trigger system. One is called *cosmic veto trigger*, which is designed to reduce the trigger rate by removing the cosmic ray events which comprise almost all of the triggered events by the neutral trigger. This trigger is developed in order to save events with the energy less than 4.0 GeV without additional increase of the trigger rate. Now the threshold energy for the BCL in the energy trigger system is set to be 2 GeV.

The other is called *muon trigger*, which requires the back-to-back muon event using the barrel muon chamber signals. This trigger is used to check the inefficiency of the present trigger system.

3.4 Data acquisition system

The TOPAZ data acquisition system consists of an online computer (VAX-11/780) and the CAMAC-FASTBUS system. The block diagram of the system is shown in Fig.3.22. Since the TPC had larger data size than other detectors, the data acquisition was separated into the TPC and the non-TPC parts. The data acquisition sequence, which was controlled by an interrupt control system(ICS), a kind of micro-processor system on FASTBUS, was complicated in order to reduce dead time in spite of the large data size of the TPC ($\sim$ 100 kb/event).

The electric analog signals form the TOPAZ detector start to be digitized by the beam crossing over signal (BC/O). When the trigger is issued, the ICS starts reading non TPC data. Then the ICS sends their data to an online computer VAX-11/780. The data from the TPC is digitized in parallel with this sequence. After the all TPC data were digitized, the ICS sends trigger system a reset signal to be ready to next BC/O and send the TPC data to VAX from local buffers.

The data taken by the VAX was then send to the TRISTAN central computer, FACOM M-1800, via an optical fiber link by the VAX-FACOM interface (DACU). This offline computer carries out the rearrangement of the data format and quick analysis to check the data acquisition system. To monitor environmental condition, such as temperatures, pressures, gas flow rates, high voltage, currents, and magnetic field, a μ-PDP 11/73 computer is employed to read them. These data are transferred to the online computer, and are stored in the record.

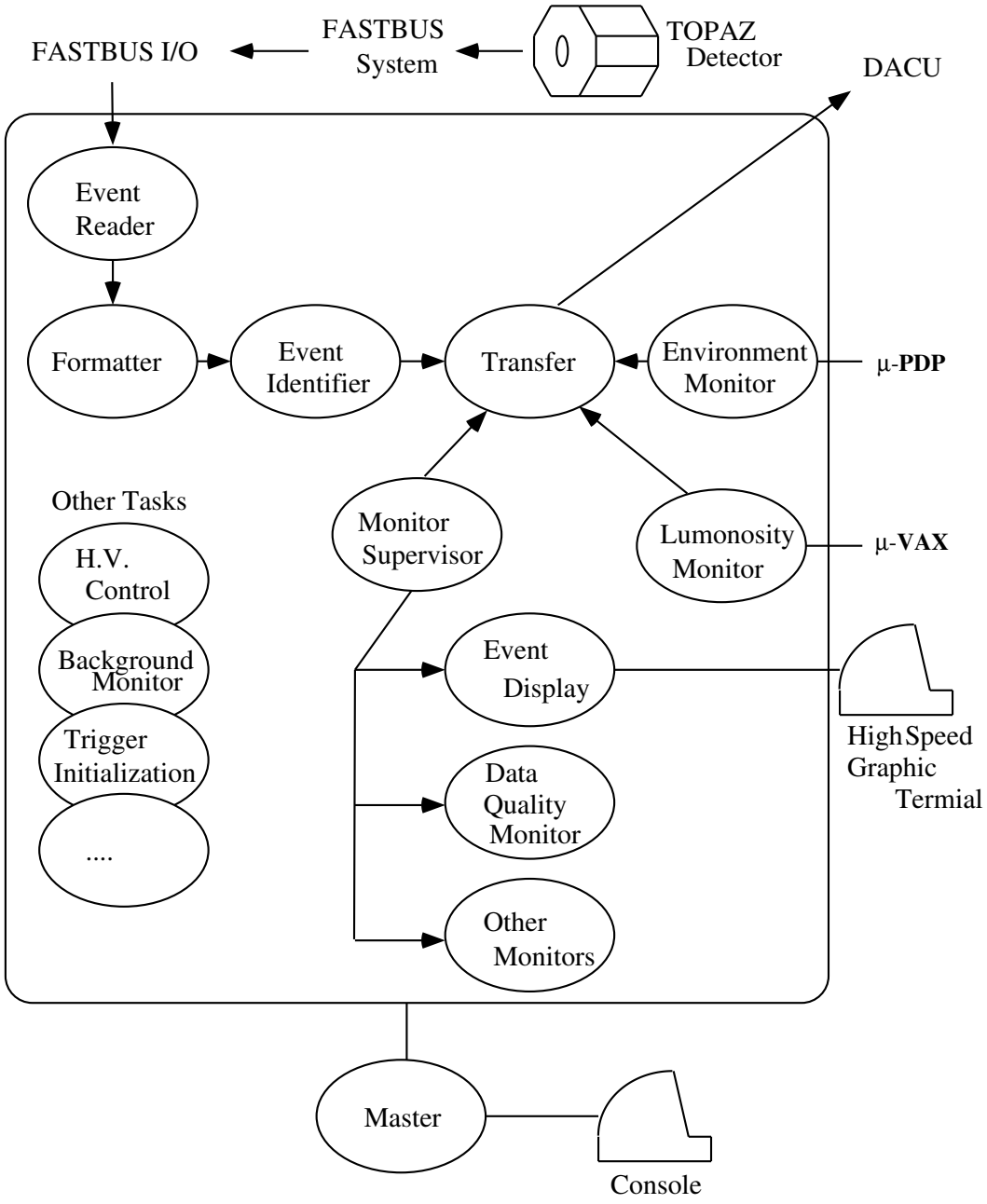

Figure 3.22: The tasks working on the online computer, VAX-11/780.